

High Electron Mobility in Vacuum and Ambient for PDIF-CN₂ Single-Crystal Transistors

Anna S. Molinari,^{*,†} Helena Alves,[‡] Zhihua Chen,[§] Antonio Facchetti,^{*,§} and Alberto F. Morpurgo^{*,||}

Kavli Institute of Nanoscience, Delft University, Lorentzweg 1, 2628CJ, Delft, The Netherlands, INESC-MN, Rua Alves Redol 9, 1000-029 Lisboa, Portugal, Polyera Corporation, 8025 Lamon Avenue, Skokie, Illinois 60077, and DPMC and GAP, University of Geneva, 24 Quai Ernest-Anserment CH-1211, Geneva, Switzerland

Received December 17, 2008; E-mail: A.S.Molinari@tudelft.nl; a-facchetti@polyera.com; Alberto.Morpurgo@unige.ch

Semiconductor devices based on organic molecules are of interest for large area electronics as well as to underscore fundamental charge transport effects in molecular solids.¹ The field-effect transistor (FET, Figure 1) is an electronic device where the current between the source and drain contacts (I_D), for a given source-drain voltage (V_{DS}), is modulated by the application of the gate-source bias (V_{GS}). In this device one of the key figures of merit is the field-effect mobility (μ_{FET}), which should be as large as possible to enable the fabrication of devices with greater performance.¹ Using the FET architecture, the carrier mobilities of several polycrystalline/amorphous p-channel (charge = hole) and n-channel (charge = electron) organic semiconductor films have been tested.² Although FETs based on polycrystalline organic semiconductor will probably be the first to be implemented into a commercial product,¹ FETs based on single-crystal organic semiconductors are far more interesting to probe ultimate charge transport efficiencies.³ To date, the greatest hole mobilities reported are for single-crystal FETs (SCFETs) based on tetracene ($\mu_{FET} \approx 2.4 \text{ cm}^2/(\text{V}\cdot\text{s})$, PDMS gate dielectric)^{3b} and rubrene ($\mu_{FET} \approx 20 \text{ cm}^2/(\text{V}\cdot\text{s})$, air-gap gate dielectric; $\mu_{FET} < 10 \text{ cm}^2/(\text{V}\cdot\text{s})$, other gate dielectrics).^{3c,d,1} Other p-channel single crystal semiconductors such as anthracene, pentacene, TIPS-pentacene, DPh-BDSe, and BPT2 exhibit μ_{FET} values = 0.02–2.2 $\text{cm}^2/(\text{V}\cdot\text{s})$.^{3e–j} Like thin-film-based FETs, single-crystal FETs based on n-channel semiconductor are far more rare and fall short in performance when compared to p-channel semiconductors. The best n-channel SCFETs reported to date were fabricated with copper perfluorophthalocyanine (FCuPc, $\mu_{FET} = 0.2 \text{ cm}^2/(\text{V}\cdot\text{s})$, parylene gate dielectric)^{3k} and tetracyanoquinodimethane (TCNQ, $\mu_{FET} = 1.6 \text{ cm}^2/(\text{V}\cdot\text{s})$ in vacuum, air-gap gate dielectric).^{3c} Despite the lower performance of thin-film as compared to single-crystal FETs, several n-channel semiconductors have shown far larger performance than FCuPc and TCNQ in thin-film-based FETs.^{2d,4} This suggests that through an appropriate choice of the molecular material, n-channel SCFETs may approach—or even exceed—the μ_{FET} of the best p-channel transistors.

Among the n-channel semiconductors for FETs, *N,N'*-bis(*n*-alkyl)-(1,7 and 1,6)-dicyanoperylene-3,4:9,10-bis(dicarboximide)s (PDIR-CN₂), have shown great potential.⁵ Some PDIR-CN₂ derivatives exhibit excellent electrical performance and remarkable environmental stability ($\mu_{FET} \approx 0.01$ –0.1 $\text{cm}^2/(\text{V}\cdot\text{s})$ for PDI8-CN₂ where R = C₈H₁₇; $\mu_{FET} \approx 0.1$ –0.6 $\text{cm}^2/(\text{V}\cdot\text{s})$ for PDIF-CN₂ where R = CH₂C₃F₇) for vapor-/solution-deposited thin-film FETs.⁵ Since it is now established that the greater structural order of single-crystalline materials enables high-quality devices with many different molecular materials,⁶ we decided to investigate single-crystal transistors based on PDIF-CN₂ which exhibits the largest thin-film μ_{FET} within the core-cyanated perylene

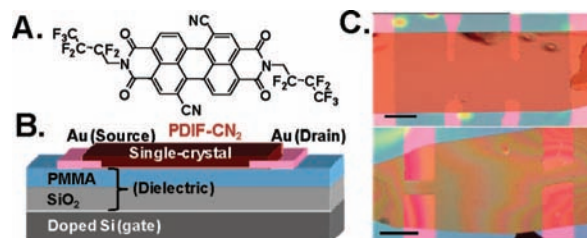


Figure 1. (A) Molecular structure of PDIF-CN₂; (B) schematic layout of a single-crystal field-effect transistor; (C) optical microscope images of PDIF-CN₂ devices used in our investigations. The bar is 200 μm .

family. Thanks to the *N*-fluorocarbon functionalization, PDIF-CN₂ is thermally stable and sublimates quantitatively, thus enabling high-quality single crystal growth by vapor phase transport. Furthermore, PDIF-CN₂ crystal structure is known.^{5b} Here we demonstrate that PDIF-CN₂-based SCFETs with PMMA as the gate dielectric exhibit $\sim 10\times$ larger mobility than the corresponding thin-film devices both in the air and in vacuum. Furthermore, other PDIF-CN₂ SCFET characteristics are also promising and include near-zero threshold voltage (V_{th}) and subthreshold slope (S) and current on/off ratio (I_{on}/I_{off}) of the same order of the very best p-channel single-crystal devices.

Single-crystal FETs (Figure 1) were fabricated by the procedure previously reported for p-channel semiconductors.^{6a} PDIF-CN₂ (Polyera ActivInk N1100) red rectangular crystals with lengths of few millimeters and widths up to 500 μm were obtained by physical vapor transport in a stream of Ar.⁷ These thin crystals ($< 1 \mu\text{m}$ thick) are difficult to handle but we were able to laminate them onto heavily doped Si(gate)/SiO₂–PMMA (dielectric) substrates with prefabricated Ti/Au (source-drain) contacts. This bottom-up approach avoids damaging the delicate surface of the organic material. The bilayer dielectric structure minimizes electron trapping by the hydroxyl groups of the SiO₂ surface.⁸ Both two- and four-terminal configurations were employed to account for the possible influence of the contact resistance. Figures 1 and S1 provide optical microscope images of some single crystal devices.

Typical electrical characteristics of PDIF-CN₂ SCFETs measured in vacuum and in air are shown in Figure 2. One of the first striking features is that they are virtually free of hysteresis and in most cases the threshold voltage is between -5 and $+5 \text{ V}$ usually close to 0 V . This value is much smaller than that measured for vapor-deposited PDIF-CN₂ thin-film transistors ($V_{th} = -20$ to ca. -30 V)^{5b} demonstrating that the dopant concentration in PDIF-CN₂ single-crystals is substantially reduced as compared to thin-films. This lower dopant concentration may be due to the enhanced chemical purity of the vapor-grown single-crystals. Another device feature that should be stressed is the linear behavior of the I_D at low V_{DS} (Figure 2A), demonstrating the absence of strong contact effects. This result is remarkable considering that high work-function gold is used as the metal contact.

[†] Delft University.

[‡] INESC-MN.

[§] Polyera Corporation.

^{||} University of Geneva.

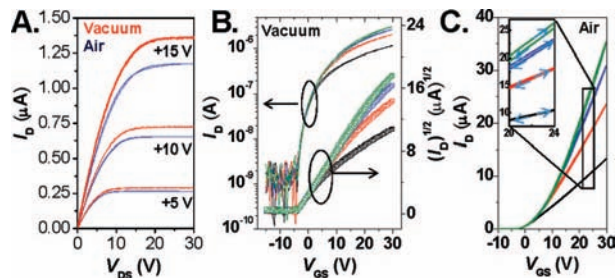


Figure 2. (A) Output plots for the same PDIF-CN₂ FET measured in vacuum (red) and in ambient (blue). (B) Transfer plot of the I_D versus V_{GS} for different values of the V_{DS} (+5 V = black, +10 V = red, +15 V = blue, and +20 V = green). The corresponding square root of I_D values are also shown in the same plot. (C) Transfer plot of the I_D versus V_{GS} measured in air for different values of the V_{DS} (+5 V = black, +10 V = red, +15 V = blue, and +20 V = green). The inset shows the negligible I - V hysteresis. For this device the crystal width W is 680 μm and the channel length $L \approx 1$ mm.

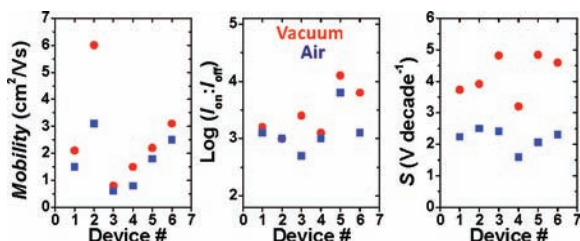


Figure 3. Electron mobilities, $I_{\text{on}}/I_{\text{off}}$, and S for six single-crystal PDIF-CN₂ FETs measured in vacuum (red) and in the air (blue).

Low workfunction metals are usually required to inject electrons in n-channel organic devices.⁹

PDIF-CN₂ electron mobility for several single-crystal devices was extracted in the linear regime according to the equation $\mu_{\text{FET}} = L/WC_1V(\partial I_D/\partial V_{GS})$, where V is the potential difference measured between the voltage probes, L their distance, W is the channel width, and C_1 is the measured capacitance-per-unit-area between gate and conduction channel. Figure 3 shows the μ_{FET} and the $I_{\text{on}}/I_{\text{off}}$ for several devices measured both in vacuum and in ambient conditions. The vacuum μ_{FET} values range from ~ 6 to 1 $\text{cm}^2/(\text{V}\cdot\text{s})$ whereas the mobility in ambient ranges between ~ 3 and 0.8 $\text{cm}^2/(\text{V}\cdot\text{s})$. Note that similar values were obtained for both two- and four-terminal measurement configurations confirming the good quality of the contacts. Interestingly, a comparable mobility reduction from vacuum to ambient ($\sim 2\times$) has recently been observed for TFT based on solution-processed or vapor-deposited polycrystalline films of PDIF-CN₂.¹⁰ However, the values obtained for single-crystals are the largest mobility values reported to date (in ambient and in vacuum). The best vacuum mobility is $\sim 4\times$ larger than the best reported for TCNQ in vacuum.³ Such mobility value is close to/larger than that of holes in rubrene SCFETs ($\mu_{\text{FET}} = 0.01$ – 10 $\text{cm}^2/(\text{V}\cdot\text{s})$)^{8,31} in devices fabricated using a gate dielectric different than air-gap ($k > 1$). Other FET parameters such as S and the $I_{\text{on}}/I_{\text{off}}$ were analyzed. In our PDIF-CN₂ devices $S = \sim 1.9$ to 5 V decade^{-1} , which is comparable to those of tetracene but larger than the best single-crystal rubrene FETs when the gate dielectric capacitance is taken into account (see Supporting Information).¹¹ Finally, the $I_{\text{on}}/I_{\text{off}}$ of PDIF-CN₂ SCFETs is $\sim 10^3/10^4$ for different devices, comparable/slightly lower than in high-quality p-channel SCFETs, but larger than that of thin-film PDIF-CN₂ FETs.^{5b}

The difference between the PDIF-CN₂ thin-film (~ 0.1 to 0.6 $\text{cm}^2/(\text{V}\cdot\text{s})$) and single-crystal (~ 1 to 6 $\text{cm}^2/(\text{V}\cdot\text{s})$) mobility values may have several origins. Efficient charge transport in organic semiconductors requires a uniform and continuous film morphology; however, vapor-/solution-deposited thin films are usually characterized by grain boundaries and random crystalline molecular orientation which limit

the device performance. A single crystal represents an almost ideal situation for charge transport characterized by absence of macroscopic grain boundaries, a very smooth and homogeneous surface, and micrometer-extended ordered molecular arrangement. Moreover, the crystal growth process provides an additional purification step reducing charge traps.

In conclusion, we demonstrated n-channel SCFETs exhibiting field-effect mobilities approaching those of the best p-channel FETs when fabricated with dielectric materials with comparable k values. These data will provide additional stimuli for the synthesis and development of chemically engineered n-channel organic semiconductors, and it will be interesting to study how this single-crystal semiconductor performs with unique dielectric materials and device architectures.¹²

Acknowledgment. We are grateful to NanoNed and NWO for financial support. H.A. also acknowledges FCT for financial support under contract no. SFRH/BPD/34333/2006.

Supporting Information Available: Single-crystal device fabrication and measurements details. This material is available free of charge via the Internet at <http://pubs.acs.org>.

References

- (1) (a) Casado, J.; Takimiya, K.; Otsubo, T.; Ramirez, F. J.; Quirante, J. J.; Ponce Ortiz, R.; Gonzalez, S. R.; Oliva, M. M.; Lopez Navarrete, J. T. *J. Am. Chem. Soc.* **2008**, *130*, 14028. (b) Kalihari, V.; Tadmor, E. B.; Greg, H.; Frisbie, C. *Adv. Mater.* **2008**, *20*, 4033. (c) Mas-Torrent, M.; Rovira, C. *Chem. Soc. Rev.* **2008**, *37*, 827. (d) Chabiniy, M. L.; Jimison, L. H.; Rivnay, J.; Salleo, A. *MRS Bull.* **2008**, *33*, 683. (e) Cornil, J.; Bredas, J.-L.; Zaumseil, J.; Sirringhaus, H. *Adv. Mater.* **2007**, *19*, 1791. (f) Locklin, J.; Roberts, M.; Mannsfeld, S.; Bao, Z. *Polym. Rev.* **2006**, *46*, 79.
- (2) (a) Zhang, M.; Tsao, H. N.; Pisula, W.; Yang, C.; Mishra, A. K.; Mueller, K. *J. Am. Chem. Soc.* **2007**, *129*, 3472. (b) Anthony, J. E. *Chem. Rev.* **2006**, *106*, 5028. (c) Landis, K. C.; Sarjeant, A.; Katz, H. E. *Chem. Mater.* **2008**, *20*, 3609. (d) Yang, C.; Kim, J. Y.; Cho, S.; Lee, J. K.; Heeger, A. J.; Wudl, F. *J. Am. Chem. Soc.* **2008**, *130*, 6444.
- (3) (a) Reese, C.; Bao, Z. *Mater. Today* **2004**, *10*, 20. (b) Podzorov, V.; Menard, E.; Borissov, A.; Kiryukhin, V.; Rogers, J. A.; Gershenson, M. E. *Phys. Rev. Lett.* **2004**, *93*, 086602. (c) Menard, E.; Podzorov, V.; Hur, S.-H.; Gaur, A.; Gershenson, M. E.; Rogers, A. *Adv. Mater.* **2004**, *16*, 2097. (d) Reese, C.; Chung, W.-J.; Ling, M.-M.; Roberts, M.; Bao, Z. *Appl. Phys. Lett.* **2006**, *89*, 202108. (e) Roberson, L. B.; Kowalik, J.; Tolbert, L. M.; Kloc, C.; Zeis, R.; Chi, X.; Fleming, R.; Wilkins, C. *J. Am. Chem. Soc.* **2005**, *127*, 3069. (f) Payne, M. M.; Parkin, S. R.; Anthony, J. E.; Kuo, C.-C.; Jackson, T. N. *J. Am. Chem. Soc.* **2005**, *127*, 4986. (g) Aleshin, A. N.; Lee, J. Y.; Chu, S. W.; Kim, J. S.; Park, Y. W. *Appl. Phys. Lett.* **2004**, *84*, 5383. (h) Zeis, R.; Kloc, C.; Takimiya, K.; Kunugi, Y.; Konda, Y.; Niihara, N.; Otsubo, T. *Jpn. J. Appl. Phys.* **2005**, *44*, 3712. (i) Ichikawa, M.; Yanagi, H.; Shimizu, Y.; Hotta, S.; Suganuma, N.; Koyama, T.; Taniguchi, Y. *Adv. Mater.* **2002**, *14*, 1272. (j) Mas-Torrent, M.; Hadley, P.; Bromley, S. T.; Ribas, X.; Tarrés, J.; Mas, M.; Molins, E.; Veciana, J.; Rovira, C. *J. Am. Chem. Soc.* **2004**, *126*, 8546. (k) Tang, Q.; Li, H.; Liu, Y.; Hu, W. *J. Am. Chem. Soc.* **2006**, *128*, 14634. (l) Hulea, I. N.; Fratini, S.; Xie, H.; Mulder, C. L.; Iosad, N. N.; Rastelli, G.; Ciuchi, S.; Morpurgo, A. F. *Nat. Mater.* **2006**, *5*, 982.
- (4) Yasuda, T.; Goto, T.; Fujita, K.; Tsutsui, T. *Appl. Phys. Lett.* **2004**, *85*, 2098.
- (5) (a) Jung, T.; Yoo, B.; Wang, L.; Dodabalapur, A.; Jones, B. A.; Facchetti, A.; Wasielewski, M. R.; Marks, T. J. *Appl. Phys. Lett.* **2006**, *88*, 183102. (b) Jones, B. A.; Ahrens, M. J.; Yoon, M.-H.; Facchetti, A.; Marks, T. J.; Wasielewski, M. R. *Angew. Chem., Int. Ed.* **2004**, *43*, 6363.
- (6) (a) de Boer, R. W. I.; Gershenson, M. E.; Morpurgo, A. F.; Podzorov, V. *Phys. Status Solidi A* **2004**, *201*, 1302. (b) Gershenson, M. E.; Podzorov, V.; Morpurgo, A. F. *Rev. Mod. Phys.* **2006**, *78*, 973.
- (7) Laudise, R. A.; Kloc, C.; Simpkins, P. G.; Siegrist, T. *J. Cryst. Growth* **1998**, *187*, 449.
- (8) (a) Todescato, F.; Capelli, R.; Dinelli, F.; Murgia, M.; Camaioni, N.; Yang, M.; Bozio, R.; Muccini, M. *J. Phys. Chem. B* **2008**, *112*, 10130. (b) Chua, L.-L.; Zaumseil, J.; Chang, J.-F.; Ou, E. C.-W.; Ho, P. K.-H.; Sirringhaus, H.; Friend, R. H. *Nature* **2005**, *434*, 194. (c) Takahashi, T.; Takenobu, T.; Takeya, J.; Iwasa, Y. *Appl. Phys. Lett.* **2006**, *88*, 033505.
- (9) Hill, I. G.; Kahn, A. *Proc. SPIE* **1998**, *3476*, 168.
- (10) (a) Piliago, C.; Jarzab, D.; Gigli, G.; Chen, Z.; Facchetti, A.; Loi, M. A. *Adv. Mater.* **2009**, in press. Burghard, H.; Dosch, M.; Jansen, K.; Kern, H. *Klausk. J. Am. Chem. Soc.* **2008**, *130*, 4637.
- (11) de Boer, R. W. I.; Klapwijk, T. M.; Morpurgo, A. F. *Appl. Phys. Lett.* **2003**, *83*, 4345.
- (12) (a) Cho, J. Ho.; Lee, J.; Xia, Y.; Kim, B. S.; He, Y.; Renn, M. J.; Lodge, T. P.; Frisbie, C. *Nat. Mater.* **2008**, *7*, 900. (b) Mannsfeld, S. C. B.; Sharei, A.; Liu, S.; Roberts, M. E.; McCulloch, I.; Heeney, M.; Bao, Z. *Adv. Mater.* **2008**, *20*, 4044. (c) Liu, S. G.; Mannsfeld, S. C. B.; Wang, W. M.; Sun, Y.-S.; Stoltenberg, R. M.; Bao, Z. *Chem. Mater. ACS ASAP*. (d) Salleo, A.; Arias, A. *Adv. Mater.* **2007**, *19*, 3540.

JA809848Y